



Strathprints Institutional Repository

Li, Maodeng and Jing, Wuxing and Macdonald, Malcolm and McInnes, Colin (2011) *Adaptive backstepping control for optimal descent with embedded autonomy*. *Aerospace Science and Technology*, 15 (7). pp. 1396-1411. ISSN 1270-9638

Strathprints is designed to allow users to access the research output of the University of Strathclyde. Copyright © and Moral Rights for the papers on this site are retained by the individual authors and/or other copyright owners. You may not engage in further distribution of the material for any profitmaking activities or any commercial gain. You may freely distribute both the url (<http://strathprints.strath.ac.uk/>) and the content of this paper for research or study, educational, or not-for-profit purposes without prior permission or charge.

Any correspondence concerning this service should be sent to Strathprints administrator: <mailto:strathprints@strath.ac.uk>

Adaptive Backstepping Control for Optimal Descent with Embedded Autonomy

Maodeng Li*, Wuxing Jing

*Department of Aerospace Engineering, Harbin Institute of Technology, Harbin,
Heilongjiang, 150001, China*

Malcolm Macdonald, Colin R McInnes

*Advance Space Concepts Laboratory, University of Strathclyde, Glasgow, Scotland, G1
1XJ, E.U.*

Abstract

Using Lyapunov stability theory, an adaptive backstepping controller is presented in this paper for optimal descent tracking. Unlike the traditional approach, the proposed control law can cope with input saturation and failure which enables the embedded autonomy of lander system. In addition, this control law can also restrain the unknown bounded terms (i.e., disturbance). To show the controller's performance in the presence of input saturation, input failure and bounded external disturbance, simulation was carried out under a lunar landing scenario

Keywords:

Adaptive backstepping control, Input failure, Input saturation, Optimal descent

*Corresponding author

Email address: mdeng1985@gmail.com (Maodeng Li)

1. Introduction

Over the past four decades, many studies on the guidance of planetary descent have been extensively reported in the literature [1–6]. Among those approaches, the tangent optimal guidance law [4, 5, 7–9] has been investigated widely. The advantage of this steering law is that it is derived from optimal control theory, therefore it can achieve fuel optimal (suboptimal). In general, a closed form solution for this guidance law cannot be found for the full model [5]. An effective method to approach the optimal solution is restricting the acceleration profile in a polynomial function in each axis [4, 5, 7], the analytic equations of velocity and position can be integrated from the acceleration profile. Therefore, the guidance acceleration can be solved from boundary conditions. Another method is developing a closed form solution for the simplified model of the full model initially, and then designing a control law to track the developed closed form solution [8, 9].

However, much of above-mentioned works assume the actuator to work perfectly. In fact, the actuator is often subjected to saturation, while actuator failure may also occur. Therefore, the derivation of a controller for planetary optimal descent in the presence of input saturation and failure is an important issue.

To connect the theory studies and engineering practice, this paper proposes an adaptive backstepping control law to track the optimal descent orbit and attitude trajectories. It is shown that this control law is robust against the input saturation and unknown bounded disturbance. Such a control law enables the concept of embedded autonomy within lander system as it is able to cope with thruster failures without requiring the on-board monitoring

systems.

The rest of this paper is organized as follows: In Section 2, the dynamics of the descent are presented. In addition, the optimal linear tangent law and a closed form solution based on a simplified model are also introduced in Section 2. Section 3 develops an adaptive backstepping controller for a class of nonlinear system with multiple input in the presence of input saturation and failure. Thereafter, the optimal descent control law is illustrated in Section 4. Section 5 shows the simulation results and discussion. Finally, conclusions are provided in Section 6.

2. Optimal Descent

The dynamics of descent can be described as follows [4],

$$\dot{r} = -w \quad (1a)$$

$$\dot{\phi} = \frac{1}{r}u \quad (1b)$$

$$\dot{\lambda} = \frac{1}{r \cos \phi}v \quad (1c)$$

$$\dot{u} = -\frac{v^2}{r} \tan \phi + \frac{uw}{r} + \frac{T_x}{m} \quad (1d)$$

$$\dot{v} = \frac{uv}{r} \tan \phi + \frac{vw}{r} + \frac{T_y}{m} \quad (1e)$$

$$\dot{w} = -\frac{u^2 + v^2}{r} + \frac{\mu}{r^2} + \frac{T_z}{m} \quad (1f)$$

$$\dot{m} = -T/(I_{sp}g_E) \quad (1g)$$

where, μ is the planetary gravitational constant, $[r, \phi, \lambda]^\top$ describes the lander's position with the polar form, $V = [u, v, w]^\top$ describes the lander's

velocity in vehicle carried local vertical frame \mathbb{F}_H [9],

$$\begin{bmatrix} T_x \\ T_y \\ T_z \end{bmatrix} = \begin{bmatrix} -T \cos \alpha_B \cos \psi_B \\ -T \cos \alpha_B \sin \psi_B \\ -T \sin \alpha_B \end{bmatrix} \quad (2)$$

is the thrust vector expressed in \mathbb{F}_H , T is the thrust vector magnitude, ψ_B is lander's yaw angle, α_B is lander's pitch angle, m is the lander's mass, Eq. 1g is the mass flow equation with I_{sp} the lander's specific impulse (impulse per unit weight-on-Earth of propellant) and g_E the gravitational acceleration on the Earth's surface.

For a landing mission in which boundary height and velocity are specified, it is well known that the tangents of the optimal attitude angles are linear functions of time which can be described as follows [4, 5],

$$\tan \psi_B = a_1 \quad (3a)$$

$$\tan \alpha_B = a_2 t + a_3 \quad (3b)$$

where, a_i ($i = 1, 2, 3$) are unknown constants to be solved.

Neglecting small terms $-v^2/r \tan \phi$, uw/r , $uv/r \tan \phi$, and uw/r in Eq. (1) which are high-order terms in the normalized form, expanding the dimensionless thrust acceleration and gravitational acceleration, and the cosine of attitude vertical angle to a high-order polynomial, the optimal landing

trajectory can be solved as a closed form [9],

$$u_d(t) = \sum_{i=0}^n u_i t^i \quad (4a)$$

$$v_d(t) = a u_d(t) \quad (4b)$$

$$w_d(t) = \sum_{i=0}^{n-1} w_i t^i \quad (4c)$$

$$h_d(t) = \sum_{i=0}^n h_i t^i \quad (4d)$$

where u_i , w_i , and h_i are functions of unknown constants a_i ($i = 1, 2, 3$), and subscript d indicates desired values. Therefore, the unknown constants a_i ($i = 1, 2, 3$) can be solved from boundary conditions of height and velocity and the closed form guidance trajectory can be solved as well.

3. Adaptive Backstepping Control

The backstepping control law is well suited to spacecraft slew control [10–12]. However, few of them addressed the problem of input saturation and failure. In [13], an adaptive backstepping control was developed to cope with input saturation. But it is only for a single input system which limits its application. In this section, a general adaptive backstepping control law for a class of system with multiple input is introduced using matrix theory and Lasalle-Yoshizawa theorem, especially for the orbit and attitude tracking of the landing system. It will be shown that this control law can be used for descent guidance and control which enables the concept of embedded autonomy to cope with input saturation and failure. In addition, it will be also shown that this control law can restrain the unknown bounded external disturbance by updating its gain to estimate the disturbance's bound.

Consider a class of dynamic systems with the form of

$$\dot{x}_1 = f_1(x_1)x_2 \quad (5a)$$

$$\dot{x}_2 = f_2(x_1, x_2) + d + B_0u \quad (5b)$$

where $x_1 \in R^{n_1}$ and $x_2 \in R^{n_2}$ are the state variables, $f_1 \in R^{n_1 \times n_2}$ is a matrix of continuously differentiable nonlinear functions, $f_2 \in R^{n_2}$ is a known smooth nonlinear function, d is a unknown bounded time-varying disturbance or an uncertain term, $u \in R^m$ is the actual control input and B_0 is the coefficient matrix of control input.

In practice, if the control input is subjected to saturation and control failure may occur, the actual input u can be written as

$$u = f_a(\text{sat}(u_c)) \quad (6)$$

where u_c is the command input, $\text{sat}(\cdot)$ is the saturation function and f_a describes the failure mode.

A control law is now required with the property that all states of the system in Eq. (5) are bounded and stable at $x_1, x_2 = 0$, i.e., $x_1, x_2 \rightarrow 0$ as $t \rightarrow \infty$.

It will be shown that the control law for command input

$$u_c = -B_0^\dagger(F_2(x_2 - p) + f_1^\top x_1 + f_2 - \dot{p} + \frac{d_{0e}^2 z_2}{\|z_2\|d_{0e} + \bar{f}_3\|z_2\|^2}) \quad (7)$$

possesses these properties, where B_0^\dagger is the Moore-Penrose pseudoinverse of B_0 (The definition of Moore-Penrose pseudoinverse can be found in Ref. [14]), F_2 is a positive definite matrix, $0 < \bar{f}_3 < \bar{f}_2$ and $\bar{f}_2 > 1/2$ is the minimum eigenvalue of F_2 , $p = -K_1 f_1^\top x_1$ and $F_1 := f_1 K_1 f_1^\top$ is a positive definite

matrix, d_{0e} is an estimate of $\|d\|$ which is obtained from

$$\dot{d}_{0e} = q\|z_2\| \quad (8)$$

where $q > 0$.

Next the derivation of the control law will be given. The following transformation is introduced to compensate the effect of input saturation and failure:

$$z_1 = x_1 - \lambda_1 \quad (9a)$$

$$z_2 = x_2 - \lambda_2 - p \quad (9b)$$

where λ_1 and λ_2 are virtual states, p is the virtual control, which is designed as,

$$p = -K_1 f_1^\top x_1 \quad (10)$$

and K_1 is chosen that $F_1 := f_1 K_1 f_1^\top$ is a positive definite matrix.

The virtual states λ_1 and λ_2 are chosen to satisfy the following equations:

$$\dot{\lambda}_1 = -F_1 \lambda_1 + f_1 \lambda_2 \quad (11a)$$

$$\dot{\lambda}_2 = -F_2 \lambda_2 - f_1^\top \lambda_1 + B_0 \Delta u \quad (11b)$$

where $\Delta u = u - u_c$ and F_2 is a positive matrix. The initial values of λ_1 and λ_2 are chosen as $\lambda_1(0) = 0, \lambda_2(0) = 0$.

The candidate of Lyapunov function is chosen as,

$$V_2 = \frac{1}{2} z_1^\top z_1 + \frac{1}{2} z_2^\top z_2 + \frac{1}{2q} \hat{d}_0^2 \quad (12)$$

where $\hat{d}_0 = d_{0e} - \|d\|$.

Substituting Eq. (10), Eq. (8), Eq. (11) and control law Eq. (7) into the derivation of V_2 along with z system, the following inequality is derived,

$$\begin{aligned}\dot{V}_2 &\leq -z_1^\top F_1 z_1 - z_2^\top F_2 z_2 + \bar{f}_3 \|z_2\|^2 \\ &\leq -\bar{f}_1 \|z_1\|^2 - (\bar{f}_2 - \bar{f}_3) \|z_2\|^2\end{aligned}\quad (13)$$

where $\bar{f}_1 > 0$ is the minimum eigenvalue of F_1 . To use LaSalle-Yoshizawa Theorem [13], the designed parameters \bar{f}_2 and \bar{f}_3 are chosen as $\bar{f}_2 > \bar{f}_3 > 0$.

Using LaSalle-Yoshizawa Theorem, it is shown that

$$\lim_{t \rightarrow \infty} z_1 = \lim_{t \rightarrow \infty} (x_1 - \lambda_1) = 0 \quad (14a)$$

$$\lim_{t \rightarrow \infty} z_2 = \lim_{t \rightarrow \infty} (x_2 - p - \lambda_2) = 0 \quad (14b)$$

To see the convergence of x_1, x_2 , the candidate of Lyapunov function of $\lambda_i (i = 1, 2)$ system is chosen as,

$$V_\lambda = \frac{1}{2} \lambda_1^\top \lambda_1 + \frac{1}{2} \lambda_2^\top \lambda_2 \quad (15)$$

Then, the derivative of V_λ along Eq. (11) can be given by

$$\dot{V}_\lambda = -\lambda_1^\top F_1 \lambda_1 - \lambda_2^\top F_2 \lambda_2 + \lambda_2^\top B_0 \Delta u \quad (16)$$

If no input saturation and failure occur, $\Delta u = 0$. Using LaSalle-Yoshizawa Theorem, it is shown that $\lim_{t \rightarrow \infty} \lambda_1 = 0$ and $\lim_{t \rightarrow \infty} \lambda_2 = 0$. Then, from Eq. (14a) it is seen that $\lim_{t \rightarrow \infty} x_1 = 0$. Thereafter, from Eq. (10) it is seen that $\lim_{t \rightarrow \infty} p = 0$. Then from Eq. (14b), it is shown that $\lim_{t \rightarrow \infty} x_2 = 0$ since $p, \lambda_2 \rightarrow 0$ as $t \rightarrow \infty$. Therefore, the asymptotic tracking is assured.

If input saturation and failure occur, $\Delta u \neq 0$. To show boundedness of λ_1 and λ_2 , Eq. (16) can be written as,

$$\dot{V}_\lambda = -\lambda_1^\top F_1 \lambda_1 - \lambda_2^\top F_2 \lambda_2 + \lambda_2^\top B_0 \Delta u \quad (17a)$$

$$\leq -\bar{f}_1 \lambda_1^\top \lambda_1 - (\bar{f}_2 - 0.5) \lambda_2^\top \lambda_2 + \frac{1}{2} (B_0 \Delta u)^\top B_0 \Delta u \quad (17b)$$

To use Lasalle-Yoshizawa Theorem, the design parameter \bar{f}_2 is chosen as $\bar{f}_2 > 0.5$ such that the second term of the above equation is negative.

Integrating Eq. (17), the following equation is given

$$\|\lambda_1\|_2 \leq \frac{1}{\sqrt{2\bar{f}_1}} \|B_0 \Delta u\| \quad (18a)$$

$$\|\lambda_2\|_2 \leq \frac{1}{\sqrt{2\bar{f}_2 - 1}} \|B_0 \Delta u\| \quad (18b)$$

From Eq. (13), it is shown that

$$\|z_1\|_2^2 = \int_0^\infty z_1^\top z_1 dt \leq \frac{1}{\bar{f}_1} V_2(0) \quad (19a)$$

$$\|z_2\|_2^2 = \int_0^\infty z_2^\top z_2 dt \leq \frac{1}{\bar{f}_2} V_2(0) \quad (19b)$$

where

$$V_2(0) = \frac{1}{2} z_1(0)^\top z_1(0) + \frac{1}{2} z_2(0)^\top z_2(0) \quad (20)$$

with $z_1(0) = x_1(0)$, and $z_2(0) = x_2(0) - A_1 f_1^\top x_1(0)$.

From Eq. (18) and Eq. (19), the bounds of the transient tracking errors can be written as

$$\|x_1\|_2 \leq \frac{1}{\sqrt{2\bar{f}_1}} (\sqrt{2V_2(0)} + \|B_0 \Delta u\|) \quad (21a)$$

$$\|x_2\|_2 \leq \frac{1}{\sqrt{\bar{f}_2}} \sqrt{V_2(0)} + \frac{1}{\sqrt{2\bar{c}_2}} \|B_0 \Delta u\| + \|A_1 f_1^\top\| \|x_1\| \quad (21b)$$

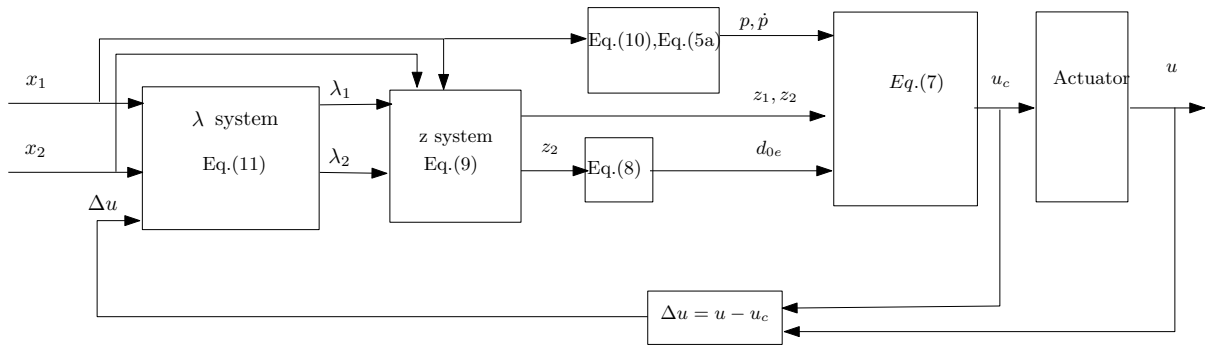


Figure 1: Flow chart of the implementation of the controller

Furthermore, the performance of control can be improved by increasing the parameters \bar{f}_1 and \bar{f}_2 . For sufficiently large \bar{f}_1 and \bar{f}_2 , then $x_1, x_2 \rightarrow 0$ as $t \rightarrow \infty$.

The flow chart of the implementation of the controller is shown in Fig. 1. Firstly, the values λ_i ($i=1,2$) are integrated from Eq.(11). The values of p and \dot{p} are calculated from Eq. (10) and Eq. (5). Thereafter, the values of z_i ($i=1,2$) and d_{0e} can be calculated from Eq. (9) and Eq. (8), respectively. Therefore the controller Eq. (7) can be implemented. The robustness against bounded external disturbance in the controller design can be seen in Eq. (7) and Eq. (8). As seen from Eq. (7), the bound of the disturbance ($\|d\|$) is an estimated parameter in the controller, and the implementation of controller does not depend on the exact value of $\|d\|$ but its estimation $\|d_{0e}\|$. The proposed controller can cope with the bounded time-varying external disturbance by updating the parameter $\|d_{0e}\|$ from Eq. (8) although the exact value of $\|d\|$ is unknown.

4. Optimal Descent Control Law

Now that the general control law has been presented, an adaptive backstepping control law is developed. The design of navigation system is not considered in this paper. It is assumed that the values of states can be obtained from the inertial navigation system and the control law is to track the predefined profile in Eq. (4).

For the orbit tracking, a height error and velocity error are defined as $e_h(t) = h(t) - h_d(t)$ and $e_v(t) = V(t) - V_d(t)$, respectively. Then the error equation of height and velocity can be written as,

$$\dot{e}_h(t) = a_h e_v(t) \quad (22a)$$

$$\dot{e}_v = d_o - 1/m u_o \quad (22b)$$

where $a_h = [0, 0, -1]$, d_o is nonlinear terms, and

$$u_o = \begin{bmatrix} T \cos \alpha_B \cos \psi_B - T_d \cos \alpha_{Bd} \cos \psi_{Bd} \\ T \cos \alpha_B \sin \psi_B - T_d \cos \alpha_{Bd} \sin \psi_{Bd} \\ T \sin \alpha_B - T_d \sin \alpha_{Bd} \end{bmatrix} \quad (23)$$

The saturation function can be written as

$$sat(u_{co}) = \begin{cases} (u_{co} + u_{norm})T_{max}/T - u_{norm} & |u_{co} + u_{norm}| \geq T_{max} \\ u_{co} & |u_{co} + u_{norm}| < T_{max} \end{cases} \quad (24)$$

where u_{co} is the command input for orbit tracking, T_{max} is the saturation level of thrust and u_{norm} is the nominal control input which can be described as follows,

$$u_{norm} = \begin{bmatrix} T_d \cos \alpha_{Bd} \cos \psi_{Bd} \\ T_d \cos \alpha_{Bd} \sin \psi_{Bd} \\ T_d \sin \alpha_{Bd} \end{bmatrix} \quad (25)$$

Furthermore, if 30% of thrust is assumed to fail at the midpoint of descent, the actual thrust level equals command thrust level when $t \leq t_f/2$ and the actual thrust level is 70% of the command thrust when $t_f/2 < t \leq t_f$. Using the special continues function \tan^{-1} to approach this characteristic, the failure mode can be written as [3],

$$f_a = \frac{1 + T_a}{2} \left(1 - \frac{2}{\pi} \frac{1 - T_a}{1 + T_a} \tan^{-1}(2t - t_f)\right) (u_{co} + u_{norm}) - u_{norm} \quad (26)$$

where $T_a = 0.7$.

It is shown that Eq. (22) is of the form of Eq. (5) with $x_1 = e_h$, $x_2 = e_v$, $f_1 = a_h$, $f_2 = 0$, $d = d_o$ and $B_0 = -1/m$. Then the controller Eq. (7) and update law Eq. (8) can be implemented directly.

For the numerical simplicity of the on-board real time computations, quaternion is used for the attitude tracking. The quaternion from \mathbb{F}_H to body frame \mathbb{F}_B [9] is defined as $Q = [q_0, q^\top]^\top$, where q_0 is a scalar part of the quaternion, and $q = [q_1, q_2, q_3]^\top$ is the vector part. The reference frame of attitude corresponding to the commanded motion is denoted by \mathbb{F}_{Bd} and its attitude with respect to \mathbb{F}_H is specified by the unit quaternion $Q_d = [q_{0d}, q_d^\top]^\top$ which is transformed from the Euler angles derived from orbit tracking system using Eq. (5.13) and Eq. (5.38) in Ref. [15]. The error of quaternion $e_Q := [e_{q0}, e_q^\top]^\top$ and angular velocity of lander are then defined as [10] $e_Q = \bar{Q}_d \otimes Q$ and $e_\omega = \omega - L(e_Q)\omega_d$, respectively, where $\bar{Q}_d = [q_{0d}, -q_d^\top]^\top$ is the inverse of Q_d and $L(e_Q)$ is the rotation matrix from \mathbb{F}_{Bd} to \mathbb{F}_B . The attitude tracking control objectives are $\lim_{t \rightarrow \infty} e_\omega = 0$ and $\lim_{t \rightarrow \infty} e_Q = [1, 0, 0, 0]^\top$. It is noted that the error quaternion should be of unit length. Therefore the attitude tracking objectives can be simplified as $\lim_{t \rightarrow \infty} [e_q; e_\omega] = 0$. Using the similar approach of [16], the error attitude

dynamics and kinematics can be expressed as,

$$\dot{e}_q = \frac{1}{2}[e_{q0}I_3 + S(e_q)]e_\omega \quad (27a)$$

$$\dot{e}_\omega = -J^{-1}(C_r\omega + n_r) - n_{do} + J^{-1}M + J^{-1}d_M \quad (27b)$$

where, J is the inertia matrix of lander, $S(\bullet)$ is cross-product operator [10], M is the control torque,

$$\begin{aligned} C_r(\omega) &= JS(L_{BH}\omega_{HP}^H) - S(J(\omega + L_{BH}\omega_{HP}^H)) + S(L_{BH}\omega_{HP}^H)J \\ n_r(\omega) &= S(L_{BH}\omega_{HP}^H)J(L_{BH}\omega_{HP}^H) + JL_{BH}\frac{d\omega_{HP}^H}{dt} + \dot{J}(\omega + L_{BH}\omega_{HP}^H) \\ n_{do} &= S(e_\omega)L(e_Q)\omega_d + L(e_Q)\dot{\omega}_d \end{aligned}$$

with L_{BH} the rotation matrix from \mathbb{F}_H to \mathbb{F}_B and $\omega_{HP}^H = [\dot{\lambda} \cos \phi, -\dot{\phi}, -\dot{\lambda} \sin \phi]^\top$ the angular velocity of \mathbb{F}_H with respect to planetary fixed frame \mathbb{F}_P [9] expressed in \mathbb{F}_H , d_M is the bounded external disturbance torque. If the $J = J_0 + \Delta J$, where J_0 and ΔJ are the certain term and uncertain term of J , respectively, then the term in Eq. (27) can be also treated as unknown bounded disturbance.

If each axis of torque is subjected to saturation, the saturation function can be written as

$$sat(M_c)(i) = \begin{cases} sign(M_c(i))M_{max} & |M_c(i)| \geq M_{max} \\ M_c(i) & |M_c(i)| < M_{max} \end{cases} \quad (28)$$

where $i = x, y, z$, M_c is the command control torque and M_{max} is the saturation value of torque.

It can be seen that Eq. (27) is of the form of Eq. (5) with $x_1 = e_q$, $x_2 = e_\omega$, $f_1 = 1/2[e_{q0}I + S(e_q)]$, $f_2 = -J^{-1}(C_r\omega + n_r) - n_{do}$, $B_0 = J^{-1}$, $u = M$, and $d = J^{-1}d_M$. The controller can be implemented directly as well.

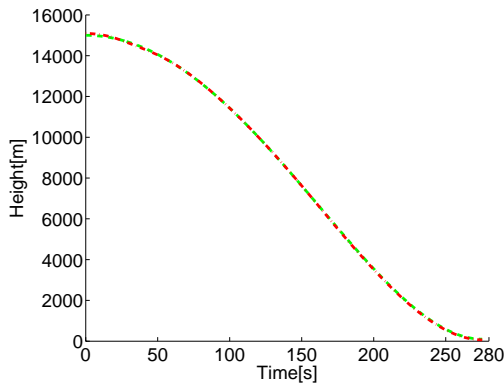
5. Results and Discussion

In this section, a numerical simulation of a sample lunar soft landing scenario is given to demonstrate the proposed control law. Nominal initial conditions of optimal descent are $h_0 = 15$ km and $V_0 = [1609.08, 100, 0]$ m/s. The initial height error is set to be 100 m and initial velocity error is set to $[2, 3, 5]^T$ m/s. Since the terminal guidance will be used following the optimal guidance, the terminal height of optimal descent is specified as $h_f = 100$ m to allow for a further study of terminal descent and the terminal velocity is specified as $V_f = [0, 0, 0]$ m/s. The assumed initial mass is 5156 kg, the nominal level of orbit thrust is 24 kN. In addition, the failure mode in Eq. (26) is adopted in numerical simulation. To compensate the thrust failures, a certain of redundancy is necessary [17]. Therefore, the saturation level of orbit thrust is chosen as 34 kN. The specific impulse of orbit thrust is $I_{sp} = 315$ s. The moment of inertia matrix is $J = \text{diag}[2.865, 1.826, 1.826] \times 10^3$ kg·m². For the attitude tracking, the initial quaternion is chosen as $Q_0 = [\sqrt{0.8}, \sqrt{0.2}, 0, 0]^T$ and the initial angular velocity is chosen as $\omega_0 = [0, 0, 0]^T$. The saturation level of control torque and the external disturbance torque are chosen as 200 Nm and $20[\cos t, \sin t, \cos 2t]^T$ Nm, respectively. The control parameters for orbit tracking are chosen as $K_1 = \text{diag}[0.1, 0.1, 0.1]$, $F_2 = \text{diag}[1, 1, 20]$, $\bar{f}_3 = 0.25$, $d_{0e}(0) = 0$, and $q = 0.01$. The control parameters for attitude tracking are chosen as $K_1 = \text{diag}[1, 1, 1]$, $F_2 = \text{diag}[5, 5, 5]$, $\bar{f}_3 = 0.1$, $d_{0e}(0) = 0$, and $q = 0.01$. The height and velocity trajectories are shown in Fig. 2. The desired trajectories and actual trajectories with adaptive backstepping control are illustrated with the dashed line and the dashdot line, respectively. Figure 3(a) shows the time history of error quaternion. The

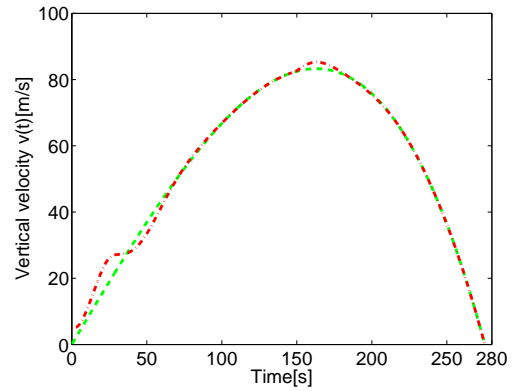
solid line represents the scalar part of the error quaternion and the dashed, dashdot, dotted line represents the vector part of the error quaternion. It can be seen that the initial state error is removed by throttling down the orbit thrusters and adjusting the values of control torques. Figure 3(b) shows the time history of the orbit thrust level. As seen from Fig. 3(b), the control law can adjust the orbit thrust level automatically after the orbit thrust failure occurs. The time history of the control torque is shown in Fig. 3(c), where the dashdot, dotted, and solid line represent the control torque in the direction of x-axis, y-axis, and z-axis, respectively. As seen from Fig. 3(c), since the control torques are mainly used to reject bounded external disturbance after transient response, the estimation of $\|d\|$ is about 20 N.m which is the exact value of $\|d\|$. Therefore, the control torques can cope with bounded external time-varying disturbance. It is also shown that the the orbit thrust saturation doesn't occur since enough redundancy is supplied to compensate the thruster failure where the control torque saturation occurs initially. However, the performance of tracking is assured since the control law can cope with thruster failure and saturation. Thus, the proposed controller enables embedded autonomy as it provides a robust approach to deal with failures without requiring the traditional Fault Detection, Isolation, and Recovery (FDIR) system.

6. Conclusions

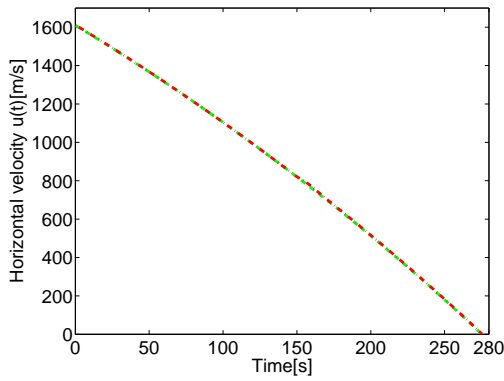
An adaptive backstepping controller for optimal descent is presented which is shown to be robust to compensate the input saturation and bounded time varying external disturbance. For practical implementation, the states



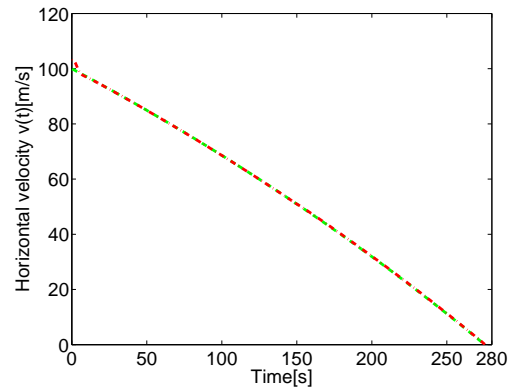
(a) Height vs time



(b) Vertical velocity: w vs time



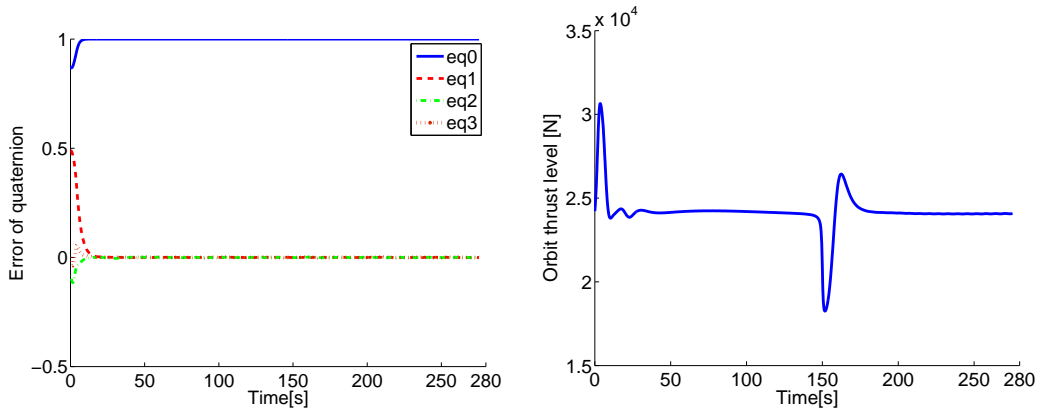
(c) Horizontal velocity: u vs time



(d) Horizontal velocity: v vs time

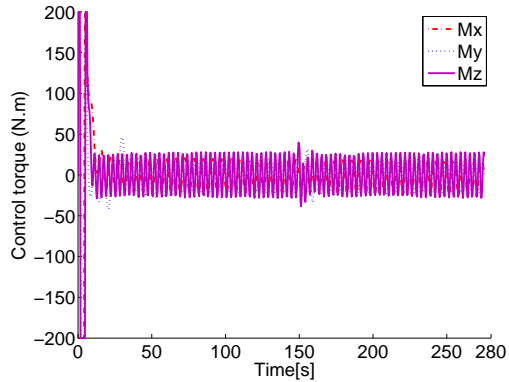
Figure 2: Numerical results of height trajectory and velocity trajectory (---, required profile; —, Adaptive backstepping Control)

can be obtained from inertial navigation system via Inertial Measurement Unit (IMU) and the estimation of the bound of disturbance and virtual state can be updated on real-time. Therefore, the proposed controller can be implemented. Such a control law is able to compensate for thruster failures without requiring the on-board monitoring systems. It offers an alternative which negates the need for the traditional Fault Detection, Isolation, and Re-



(a) Error of quaternion vs time

(b) Orbit thrust level vs time



(c) Control torque vs time

Figure 3: Numerical results of error quaternion and control input

covery (FDIR) approach through embedded autonomy. It should be noted that the proposed controller is still a theory, but one which should be better suited to implementation as it is closer to the what the system will require. It is also worth noting that by using the embedded autonomy that the real-world system is actually not that different to an ideal one as the control must autonomously correct for the ideal worlds lack of perturbations as much as it should for the real-world perturbations. The future work would focus on a

hardware-in-the-loop simulation, i.e. to run the algorithms on an actual flight processor, and perhaps in a high-fidelity simulations environment capable of performing monte-carlo campaigns.

Acknowledgments

This work has been supported by the Chinese Nature Science Foundation under grant No. 60535010.

References

- [1] R. Cheng, Lunar terminal guidance, in: Lunar Missions and Exploration, Wiley, New York, 1964.
- [2] S. Citron, S. Dunin, H. Meissinger, A terminal guidance technique for lunar landing, AIAA Journal 2 (3) (1964) 503–509.
- [3] C. McInnes, Direct adaptive control for gravity-turn descent, Journal of guidance, control, and dynamics 22 (2) (1999) 373–375.
- [4] S. Ueno, Y. Yamaguchi, 3-dimensional near-minimum fuel guidance law of a lunar landing module, in: Proceeding of AIAA Guidance, Navigation, and Control Conference, Portland, OR, 1999, pp. 248–257.
- [5] R. R. Sostaric, J. R. Rea, Powered descent guidance methods for the moon and mars, in: Proceeding of AIAA Guidance, Navigation, and Control Conference, San Francisco, California, 2005.
- [6] C. Chomel, R. Bishop, Analytical Lunar Descent Guidance Algorithm, Journal of guidance, control, and dynamics 32 (3) (2009) 915–926.

- [7] D. Wang, X. Huang, Y. Guan, GNC system scheme for lunar soft landing spacecraft, *Advances in Space Research* 42 (2008) 379–385.
- [8] H. Afshari, J. Roshanian, A. Novinzadeh, A perturbation approach in determination of closed-loop optimal-fuzzy control policy for planetary landing mission, *Proceedings of the Institution of Mechanical Engineers, Part G: Journal of Aerospace Engineering* 223 (3) (2009) 233–243.
- [9] M. D. Li, M. Macdonald, C. R. McInnes, W. X. Jing, Analytical lunar landing trajectories for embedded autonomy, *Proceedings of the Institution of Mechanical Engineers, Part G: Journal of Aerospace Engineering*(In press).
- [10] R. Kristiansen, P. Nicklasson, J. Gravdahl, Satellite Attitude Control by Quaternion-Based Backstepping, *IEEE Transactions on Control Systems Technology* 17 (1) (2009) 227–232.
- [11] C. Y. Li, W. Jing, C. Gao, Adaptive backstepping-based flight control system using integral filters, *Aerospace Science and Technology* 13 (2-3) (2009) 105–113.
- [12] I. Ali, G. Radice, J. Kim, Backstepping Control Design with Actuator Torque Bound for Spacecraft Attitude Maneuver, *Journal of guidance, control, and dynamics* 33 (1) (2010) 254–259.
- [13] J. Zhou, C. Wen, *Adaptive backstepping control of uncertain systems*, Springer, 2008.
- [14] A. Laub, *Matrix analysis for scientists & engineers*, Society for Industrial Mathematics, 2004.

- [15] B. Wie, Space vehicle dynamics and control, Reston, VA: American Institute of Aeronautics and Astronautics, Inc, 1998.
- [16] R. Kristiansen, E. Grotli, P. Nicklasson, J. Gravdahl, A model of relative translation and rotation in leader-follower spacecraft formations, *Modeling, Identification and Control* 28 (1) (2007) 3–13.
- [17] G. Tao, S. Joshi, Direct adaptive control of systems with actuator failures: state of the art and continuing challenges, in: *Proceeding of AIAA Guidance, Navigation, and Control Conference*, Honolulu, Hawaii, 2008.